A Simplified Method for (Circular) Transmission Line Model Simulation and Ultra-low Contact Resistivity Extraction

Hao Yu, Marc Schaekers, Tom Schram, Nadine Collaert, Kristin De Meyer, *Fellow*, *IEEE*, Naoto Horiguchi, Aaron Thean and Kathy Barla

Abstract—**The metal resistance in the transmission line model (TLM) structures creates a serious obstacle to determine precisely the intrinsic contact resistivity. To tackle this problem, we propose a new model, the Lump Model, to evaluate the metal resistance influence in both TLM and circular TLM (CTLM) test structures. In this work, we demonstrate the high simplicity, great robustness and flexibility of the Lump Model. The previous reported contact resistivity values extracted with CTLM are usually above 1×10^{-7} Ω·cm^2 because the metal resistance impact is commonly neglected. This is the first time that the role of the metal in CTLM is appropriately analyzed. Low contact resistivity, 3.6×10^{-8} Ω·cm^2, of standard NiSi/n-Si contact has been extracted and this shows the high sensitivity of this method.**

Index Terms—**Contact resistance, ohmic contact, transmission line model, circular transmission line model, simulation**

I. Introduction

The International Technology Roadmap for Semiconductors (ITRS) has put forward a requirement of contact resistivity below 1×10^{-8} Ω·cm^2 for the 10 nm technology node and beyond [1]. Besides this challenge, the ultra-low contact resistivity has also increased the requirement of precise measurement.

The transmission line model (TLM) [2] and the circular transmission line model (CTLM) [3] are the two most commonly applied methods to extract the contact resistivity, ρ_c, from the contact resistance, R_c. For higher values of R_c, the metal resistance impact is negligible. However, when R_c becomes lower, neglecting the metal resistance can easily lead to a misinterpretation of R_c and an inaccurate extraction of ρ_c. Marlow et al. have developed an analytical model to describe the role of the metal resistance in TLM [4]. Further, Dormaier et al. proposed a refined TLM structure to minimize the metal resistance influence [5]. Compared with TLM, CTLM benefits from its easier process and especially suits the quick contact scheme screening. However, the metal resistance influence in CTLM has never been properly analyzed.

Manuscript submitted April 6, 2014. This work was supported by imec's Core program on LOGIC DEVICES.

H. Yu and K. De Meyer are with imec, 3001 Leuven, Belgium,and also with the Department of Electrical Engineering, Katholieke Universiteit (K.U.), 3001 Leuven, Belgium (e-mail: hao.yu@imec.be).

M. Schaekers, T. Schram, N. Collaert, N. Horiguchi, A. Thean and K. Barla are with imec, 3001 Leuven, Belgium.

In this work, a simplified model, the Lump Model (LM), is designed to facilitate the simulation of the TLM and CTLM test structures. Assisted by the LM simulation, the low ρ_c of standard NiSi/n-Si contact, 3.6×10^{-8} Ω·cm^2, is successfully extracted with CTLM. Previously, the contact resistivity values extracted with CTLM were usually above 1×10^{-7} or 1×10^{-6} Ω·cm^2 [6, 7]. To our knowledge, this is the first time that the ultra-low ρ_c of metal-semiconductor (MS) contacts is properly determined by the CTLM method. The sensitivity of the CTLM method is therefore improved to be comparable with other state-of-the-art contact resistivity extraction models. [5]

II. Experiments

300 mm blanket p-type silicon wafers received an ion implantation with phosphorus (1.8 keV, 1×10^{13} cm^{-2}) and arsenic (20 keV, 3×10^{15} cm^{-2}). A post high temperature activation annealing at 1035 ºC was performed in He. CTLM patterns were defined by lithography and etching with a dielectric hardmask. A 6nm thin Ni(Pt) layer was deposited by sputtering, followed by a two-step silicidation process—a first 1 min 275 ◦C annealing in N_2 ambient was followed by a wet etching removal of Ni residue and a second 1 min 400 ◦C annealing in N_2 ambient. The standard liner stack was then deposited. Following the stack deposition, a thick layer of Cu or W was deposited by plating or by chemical vapor deposition (CVD). Chemical-mechanical planarization (CMP) was then performed until ~150nm thick metal remained. An 8nm SiC layer was deposited on Cu to prevent the oxidation. All electrical measurements were performed using an HP4156c.

III. Methodology

The top and sectional schematics of the CTLM test structure are shown in Fig. 1a. The total resistance (R_T) of CTLM is defined as the resistance between the two probes, P_1 and P_2. In reality, a four-point-probe (4pp) measurement is applied to eliminate the probe series resistance impact. R_T is measured with various spacing (s) between the metal electrodes. Two CTLM R_T-s curves of the same NiSi/n-Si contacts with the different cap metal were compared in Fig. 1b. The metal sheet resistance, R_m, on the W or Cu capped samples is ~1.5 and ~0.2 Ω/sq, respectively. A difference in R_T-s relation caused by the cap metal can be observed. Previous reports [6, 7] commonly assume that the R_T-s relation of CTLM structures is determined only by two factors—the substrate sheet resistance (R_s) and ρ_c.

However, the impact of R_m should also be included, otherwise the large deviation of the R_T-s relation caused by R_m will lead to a serious inaccuracy in the extraction of ρ_c.

Marlow et al. have developed an analytical model including the R_m influence for TLM. [4] However, because of the special pattern of CTLM test structures, there has been no analytical or numeric method to describe the role of R_m in CTLM. Alternatively, we use the TCAD simulations for the investigation of the CTLM structure. There are two major challenges for the CTLM simulation; (1) a large amount of nodes are needed for the intensive current density and complex electric field distribution and (2) the large dimension and the circular pattern. To overcome these challenges, a simplified substitute model, the Lump Model (LM), is developed to realize the simulation of both the TLM and the CTLM behavior. First, the feasibility and validity of 1D LM is checked with TLM. Then 2D LM is applied for CTLM simulation.

LM is a simple model consisting of several lumps of resistors in series to simulate the complex behavior of TLM and CTLM. The dimension and the resistance of the lumps are the two major parameters to be defined. To mimic the behavior of the TLM, LM is simply a 1D model. The construction of the LM is based on the current crowding effect at the contact edge, as illustrated by Fig. 2. The current distribution at the contact edge is derived based on the model given by Marlow et al. [4]

$$I(x) = C_1 + C_2 exp[(d-x)/a] + C_3 exp[-(d-x)/a] \quad (1)$$

where x is the distance from the edge, d is the length of the metal electrode,

$$a = \sqrt{\rho_c/(R_s+R_m)} \ ,$$
$$C_1 = R_m I(0)/(R_s+R_m) \ ,$$
$$C_2 = C_1 (R_s/R_m) exp(-d/a) \ ,$$
$$C_3 \approx -C_1 \text{ (when } d/4 \gg a) .$$

As illustrated by Fig. 2, when ρ_c is low, all the current crowds into the metal within a small area at the contact edge. We notice that, due to the current crowding effect, the distance that every piece of current flows within the substrate is almost the same, compared to the complete TLM dimension. As a result, we make an appropriate assumption that at the edge of the contact all pieces of the current travel the same distance, $\bar{L}$, along the substrate and then flow into the metal together. $\bar{L}$ can be calculated from (1)

$$\bar{L} = \int x di/I(0) = R_s L_t/(R_s+R_m) \approx L_t \ (R_m \ll R_s) \quad (2)$$

where L_t is the well-known transfer length of the TLM structure

$$L_t = \sqrt{\rho_c/R_s} \ . \quad (3)$$

The complete TLM structure can thus be simplified into three lumps in series—two metal lumps with the sheet resistance of R_m and one semiconductor lump in between with the sheet resistance R_s. The lengths of the metal lump and the semiconductor lump are $d - L_t$ and $s + 2L_t$, respectively. In LM, the role of ρ_c is represented by L_t, as shown by (3). As a result, LM is essentially a simulation model including all three factors of ρ_c, R_s and R_m. The inset of Fig.2 schematically shows the TLM and the LM structures.

To verify the robustness of both the LM and the complete TLM structure simulations, the R_T-s relations are examined and compared with the numerical model developed by Marlow et al. [4]. At the same time, the role of R_m in the TLM structure is studied. We will look at the example of $\rho_c = 1\times10^{-8}\ \Omega\cdot cm^2$ and R_s = 205 Ω/sq using three R_m values—0, 0.2, and 2.0 Ω/sq. A 100 μm electrode length and a set of spacing values are applied. As shown in Fig. 3, a good agreement is achieved between simulation and calculation. In practice, the LM simulation dramatically reduces the computation time needed as compared to the complete TLM simulation. As for the role of metal resistance, R_m causes an upwards shift of the R_T–s curve. A high R_m can even dominate the intercept of the curve.

After the verification of using a 1D LM to simulate the TLM behavior, it is clear that we can distinguish the metal and the semiconductor contribution with independent lumps. This simplification dramatically reduces the simulation complexity. As for CTLM, the simulation of a complete structure is much more difficult to realize. The major challenge is to analyze the current and field distribution in the large 3D pattern. Fortunately, we notice that, similarly with TLM, the transfer of current between the metal and the semiconductor in CTLM only happens at the contact edge and we can thus also separate the metal and semiconductor parts with a 2D LM. The settings of the 2D LM parameters are shown in Fig. 4a. The parameter L_{t1} and L_{t2} are the transfer length inside and outside the ring, respectively. Due to the fact that the radius of the circular electrode (r) is far larger than the transfer length, L_{t1} and L_{t2} are almost the same and can be both derived by (3). [4] Fig. 4b shows the R_T–s curves derived by 2D LM simulation. R_s = 205 Ω/sq and $\rho_c = 1\times10^{-8}\ \Omega\cdot cm^2$ are applied in simulation. In the ideal case, R_m = 0 and the inner and outer metal electrodes are equipotential. The voltage drops totally over the semiconductor channel and contacts of CTLM. But in reality, the resistance of the metal electrode will also cause a voltage drop. Fig. 4c and Fig. 4d show the electric potential contour plots when R_m = 0.2 Ω/sq and R_m = 2 Ω/sq. As shown in Fig. 4d, when R_m is high, the large voltage drop over the metal can suppress the effective voltage drop on the ring. Like in the TLM case in Fig. 3, R_m causes an upward shift of the CTLM R_T-s curves in Fig. 4b,.

In previous contact studies [6,7], for both TLM and CTLM, R_T-s curves are usually interpreted with only R_s and ρ_c. From the intercept, ρ_c is extracted. However, as shown by Fig. 3 and Fig. 2b, neglecting the metal influence will eventually lead to a serious inaccuracy of the ρ_c extraction, especially with high R_m (>1 Ω/sq). With simulation, the role of R_m in both TLM and CTLM can be analyzed and the ρ_c extraction can be refined. Nevertheless, R_m still serves as a parasitic factor and should be minimized to enhance the sensitivity of the ρ_c test structure. Therefore, we have switched the cap metal from W (~1.5 Ω/sq) to Cu (~0.16 Ω/sq).

Assisted by the 2D LM simulation, the CTLM R_T–s curves can successfully be derived with values of ρ_c, R_s and R_m. A new ρ_c extraction method can be developed based on electrical measurements and simulations. In the practical experiments, R_m and R_T–s data sets can be derived using the 4pp measurement. Then by modulating the R_s and ρ_c parameter values in the 2D LM, the trend of the measured R_T–s data sets can be simulated and the intrinsic R_s and ρ_c values can be determined. To examine this method, we applied it to the standard low-ρ_c NiSi/nSi contact with 150nm Cu cap. R_m and six sets of R_T-s

values were measured. In this case, R_m is 0.16 Ω/sq. Both the measurement results and the simulation curves are shown in Fig.5. For both dimensions of the CTLM, $\rho_c = 3.6\times10^{-8}$ Ω·cm^2 and R_s = 118.6 Ω/sq are determined, which shows high sensitivity of our ρ_c extraction method. For silicide contacts, two additional factors caused by silicidation are neglected in the ρ_c extraction procedures above—the lateral penetration of NiSi and the dopant segregation. The influence of both factors is small since the Ni(Pt)Si layer in our experiment is as thin as ~11 nm. Accounting for the mixed effects of these two factors, small changes can be made in the 2D LM simulation and there would be a correction of approximately $\pm0.4\times10^{-8}$ Ω·cm^2 from the ρ_c results above.

IV. CONCLUSION

The simple and robust Lump Model was presented to facilitate the simulation of both TLM and CTLM. Based on the Lump Model simulation, the total resistance-spacing (R_T-s) relations of CTLM were derived successfully including the influence of the metal. From the simulations it is clear that the metal sheet resistance needs to be reduced as much as possible thereby favoring metals like Cu and Al. Furthermore, we have developed a ρ_c extraction method combined with the Lump Model simulation, which can be used to determine ultra-low contact resistivities from the CTLM structures. The method has been demonstrated for a NiSi/n-Si contact with a ρ_c of 3.6×10^{-8} Ω·cm^2. To our knowledge, this is the lowest ρ_c that has been reliably extracted using CTLM structures. This is also the first time that the R_m impact in CTLM is successfully analyzed.

[1] *The International Technology Roadmap for Semiconductors (ITRS)*, 2013
[2] G. K. Reeves, "Specific contact resistance using a circular transmission line model", *Solid-State Electron.*, vol. 23, pp. 487-490, 1980
[3] G. K. Reeves and H. B. Harrison, "Obtaining the specific contact resistance from transmission line model measurements", *IEEE Electron Device Lett.*, vol. EDL-3, no. 5, May 1982
[4] G. S. Marlow and M. B. Das, "The effets of contact size and non-zero metal resistance on the determination of specific contact resistance", *Solid-State Electron.*, vol. 25, no. 2, pp. 91-94, 1982
[5] R. Dormaier and S. E. Mohney, "Factors controlling the resistance of ohmic contacts to n-InGaAs", *J. Vac. Sci. Technol. B*, vol. 30, no. 3, pp. 031209-1-031209-10, May/Jun 2012
[6] A. Firrincieli, K. Martens, R. Rooyackers, et al., "Study of ohmic contacts to n-type Ge: snowplow and laser activation", *Appl. Phys. Lett.*, vol. 99, pp. 242104-1-142104-3, Dec. 2011
[7] F. Liu, B. Hsia, C. Carraro, et al., "Enhanced ohmic contact via graphitization of polycrystalline silicon carbide", *Appl. Phys. Lett.*, vol. 97, pp. 262107-1-262107-3, Dec. 2010

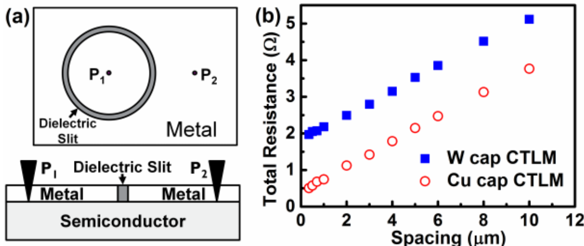

Fig. 1. (a) The schematic top view and sectional view of the CTLM test pattern. P_1 and P_2 are the probes of the current source. (b) CTLM R_T-s curves of NiSi/n-Si contacts with Cu and W cap layers. The spacing is the distance between metal electrodes.

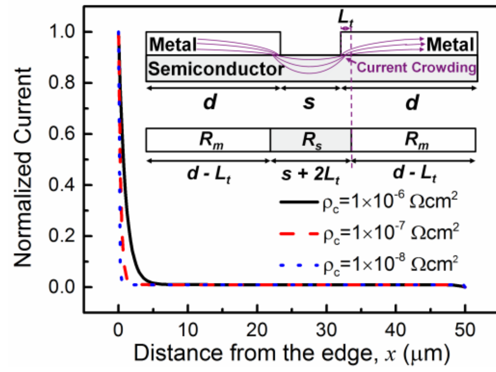

Fig.2. The normalized current in the substrate along the contact of TLM. The insets are the schematics of the complete TLM structure and LM.

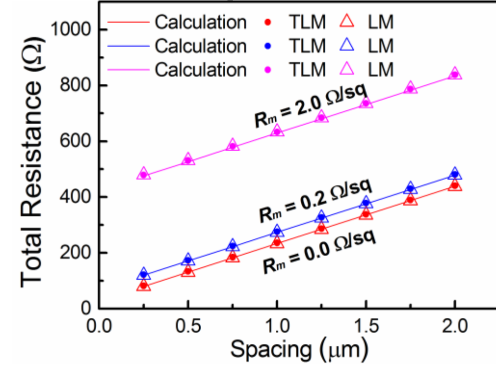

Fig. 3. The R_T-s curves derived by the numerical calculation, the complete TLM simulation and the LM simulation.

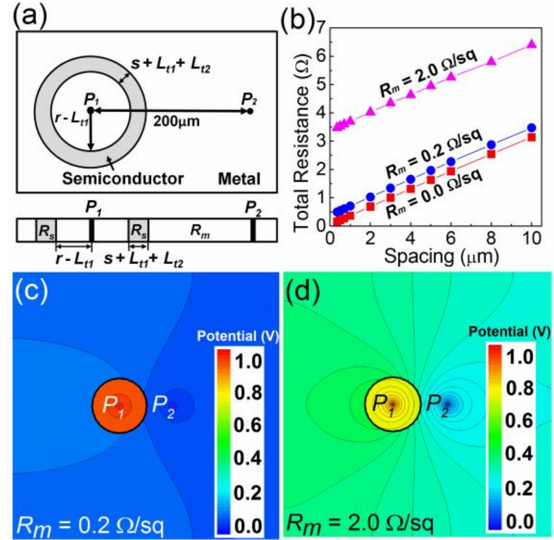

Fig. 4. (a) Schematic top view of the 2D LM and parameter settings. P_1 and P_2 are the current source positions. (b) R_T-s curves based on 2D LM simulation. And potential contour plot of CTLM simulated with 2D LM when (c) R_m = 0.2 Ω/sq, and (d) R_m = 2.0 Ω/sq.

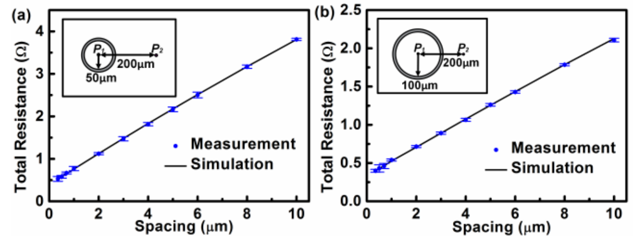

Fig. 5. The measurement and the 2D LM simulation results for CTLM of two dimensions—the circle inner radius is (a) 50μm and (b) 100μm, respectively. The short error bars exhibit the high repeatability of the measurements. The insets are the schematic top views of the CTLM structures.